Research Square

Preprints are preliminary reports that have not undergone peer review.
They should not be considered conclusive, used to inform clinical practice,
or referenced by the media as validated information.

Shotgun metagenomics reveals significant gut microbiome features in different grades of acute pancreatitis

Shanshan Yu
Peking Union Medical College Hospital&Peking Union Medical College&Chinese Academy of Medical Science and Peking Union Medical College

Yangyang Xiong
Peking Union Medical College Hospital&Peking Union Medical College&Chinese Academy of Medical Science and Peking Union Medical College

Yangyang Fu
Peking Union Medical College Hospital&Peking Union Medical College&Chinese Academy of Medical Science and Peking Union Medical College

Guorong Chen
Peking Union Medical College Hospital&Peking Union Medical College&Chinese Academy of Medical Science and Peking Union Medical College

Huadong Zhu
Peking Union Medical College Hospital&Peking Union Medical College&Chinese Academy of Medical Science and Peking Union Medical College

Xun Mo
The Second People's Hospital of Guiyang City

Jun Xu
Peking Union Medical College Hospital&Peking Union Medical College&Chinese Academy of Medical Science and Peking Union Medical College

Dong Wu (wudong@pumch.cn)
https://orcid.org/0000-0001-6439-3761

Research

Keywords: acute pancreatitis, severity, shotgun metagenomics, gut microbiota, microbiota composition dysbiosis, microbiota functional dysfunction

Posted Date: June 15th, 2020

DOI: https://doi.org/10.21203/rs.3.rs-34718/v1

License: This work is licensed under a Creative Commons Attribution 4.0 International License.
Read Full License

Version of Record: A version of this preprint was published at Microbial Pathogenesis on May 1st, 2021.
See the published version at https://doi.org/10.1016/j.micpath.2021.104849.

Abstract

Background: Acute pancreatitis (AP) has a broad spectrum of severity and is associated with considerable morbidity and mortality. We aimed to evaluate the composition and functional effects of gut microbiota in different grades of AP severity.

Results: Gut microbiota in AP patients was characterized by decreased species richness. The most representative gut microbiota in mild acute pancreatitis (MAP), moderately severe acute pancreatitis (MSAP), and severe acute pancreatitis (SAP) was *Streptococcus*, *Escherichia-coli,* and *Enterococcus*, respectively. Each of the three AP-associated genera could differentiate AP from healthy control population. Representative pathways associated with the glutathione metabolism, lipopolysaccharide biosynthesis, and amino acid metabolism (valine, leucine and isoleucine degradation) were enriched in MAP, MSAP, and SAP, respectively.

Conclusions: Our findings indicate that in patients with AP, the gut microbiome composition and function are correlated with different severity of AP from a whole-genome perspective, and new changes are observed.

Background

Acute pancreatitis (AP) is the most common gastrointestinal disease that requires acute admission and causes tremendous pain and socioeconomic burden [1]. The worldwide incidence of AP ranges from 4.9 to 80 cases per 100,000 individuals annually [2]. According to the Revised Atlanta Classification, AP is stratified into mild acute pancreatitis (MAP), moderately severe acute pancreatitis (MSAP), and severe acute pancreatitis (SAP) [3]. The outcome of AP patients with different severity is widely divergent. For instance, patients with MAP only need supportive care such as fluid and analgesia and recover within a few days. But in the non-mild form of AP, an inflammatory cascade usually leads to local and systemic complications, claims remarkable morbidity and mortality, and makes the management of AP challenging [4]. The pathogenetic mechanism underlying the progression of AP severity is yet to be elucidated [5].

Gut microbiota plays an essential role in maintaining immune homeostasis and the biological barrier of the intestine [6]. Under pathological conditions such as AP, perturbations to the gut microbiota could disrupt gut barrier, increase the intestinal permeability, and lead to bacterial translocation, which in turn triggers secondary infectious complications [7]. Several bacteria, including *Escherichia*, *Shigella*, *Enterococcus*, and *Enterobacteriaceae* family, have been found in the pancreas, indicating that their translocation from the gut could lead to infected pancreatic necrosis in non-mild AP[8]. Our previous work revealed different gut bacteria composition in AP patients with varying grades of severity. To be specific, *Bacteroides*, *Escherichis-Shigella*, and *Enterococcus* was the dominant gut microbiota species in MAP, MSAP, and SAP, respectively. Besides, *Anaerococcus* and *Enterococcus* were significantly increased and *Eubacterium hallii* decreased in non-mild AP patients [9]. Similar findings were also reported by Zhu Y et

al. [7]. These studies indicated a potential association between gut microbiota and AP progression. However, what remains obscure is what functional effects gut microbiota may exert upon the worsening of AP.

Shotgun metagenomic sequencing of the whole DNA provides valuable information about the functions of the microbial community [10]. The sequencing technology is used to obtain the entire genomic content of the microbiome and achieve accurate taxonomic classification and functional assignments. Also, it is able identify novel functional genes, antibiotic resistance genes, microbial pathways, and functional dysbiosis of the gut microbiome [11]. In this study we conducted metagenomic shotgun survey on microbial gut population of MAP, MSAP, SAP patients and three healthy controls, in order to characterize the AP-related composition and functional changes.

Methods

Subjects recruitment

The 2012 revised Atlanta classification stratified the clinical severity of AP patients into three categories: mild AP (MAP), moderately severe AP (MSAP), and severe AP (SAP) [3]. All the patients with a diagnosis of AP based on the 2012 Revised Atlanta Classification and admitted to Peking Union Medical College Hospital, Beijing, China were eligible for inclusion if they were enrolled within 48 hours of the onset of symptoms. A total of three MAP, three MSAP, and three SAP patients were included. None of AP patients had been treated in other hospitals before admission.

Healthy control population

The healthy control population (HCR) were three healthy volunteers (community workers and students) identified from Peking Union Medical College Hospital. They were age, gender and BMI matched to the patient population and selected after the completion of the patient study. We used the same definition of the HCR group with our previous work [9].

Exclusion criteria

AP patients and HCR were excluded if they took antibiotics, probiotics, Chinese herbs, steroids, and other substances that may affect the structure of the flora in up to eight weeks prior to sampling. Other exclusion criteria referred to patients with a history of immunodeficiency, allergy, asthma, celiac disease, colorectal cancer, diabetes, HIV, inflammatory bowel disease, irritable bowel syndrome, gastroenteritis, necrotizing enterocolitis, and arthritis [7].

Written informed consent was obtained from each participant. The institutional review boards of Peking Union Medical College Hospital approved this study (No. JS 1826).

Sample collection

Stool samples are generally considered the reference standard. However, they are not practical to obtain in patients with AP, since they are often afflicted by reduced gastrointestinal motility [12]. Thus, rectal swabs are commonly used instead, as previously described [13]. In this study, microbial DNA was extracted from fecal samples obtained through the rectal swab immediately after admission. All individuals should have an empty stomach (did not eat for 12 hours) before sample collection. The sample of healthy volunteers was collected in the morning. The timing of the rectal swab sampling of AP patients was within 24 hours after disease onset in all individuals. Detailed processes of sample collection were described elsewhere [9].

DNA extraction, library construction and metagenomics sequencing

DNA for metagenomics was extracted from fecal samples by using the E.Z.N.A.® DNA Kit (Omega Bio-tek, Norcross, GA, U.S.) according to the manufacturer's protocols. The DNA concentration and purity were quantified with TBS-380 and NanoDrop2000, respectively. DNA quality was examined with the 1% agarose gels electrophoresis system. DNA was fragmented to an average size of about 300 bp using Covaris M220 (Gene Company Limited, China) for paired-end library construction. The paired-end library was prepared by using TruSeqTM DNA Sample Prep Kit (Illumina, San Diego, CA, USA). Adapters containing the full complement of sequencing primer hybridization sites were ligated to the Blunt-end fragments. Paired-end sequencing was performed on Illumina HiSeq4000 platform (Illumina Inc., San Diego, CA, USA) at Majorbio Bio-Pharm Technology Co., Ltd. (Shanghai, China) using HiSeq 3000/4000 PE Cluster Kit and HiSeq 3000/4000 SBS Kits according to the manufacturer's instructions (www.illumina.com). All the raw metagenomics datasets have been deposited into NCBI Sequence Read Achieve database.

Sequence quality control and genome assembly

3' and 5' end was stripped using SeqPrep (https://github.com/jstjohn/SeqPrep). Low-quality reads (length<50 bp or with a quality value <20 or having N bases) were removed by Sickle (https://github.com/najoshi/sickle). Reads were aligned to the human genome (version 38) by BWA (http://bio-bwa.sourceforge.net) and any hit associated with the reads and their mated reads were removed. De bruijn-graph-based assembler SOAPdenovo (http://soap.genomics.org.cn) (version 1.06) was used to assemble short reads. K-mers, varying from 1/3~2/3 of reads length were tested for each sample. Scaffolds with a length over 500bp were retained for statistical tests; we evaluated the quality and quantity of scaffolds generated by each assembly and finally chose the best K-mer which yielded the minimum scaffold number and the maximum value of N50 and N90. Then, scaffolds with a length over 500 bp were extracted and broken into contigs without gaps. Contigs were used for further gene prediction and annotation. Open reading frames (ORFs) from each metagenomic sample were predicted using MetaGene (http://metagene.cb.k.u-tokyo.ac.jp/). The predicted ORFs with length being or over 100 bp were retrieved and translated to amino acid sequences using the NCBI translation table (http://www.ncbi.nlm.nih.gov/Taxonomy/taxonomyhome.html/index.cgi?chapter=tgencodes SG1). All sequences from gene sets with a 95% sequence identity (90% coverage) were clustered as the non-

redundant gene catalog by the CD-HIT (http://www.bioinformatics.org/cd-hit/). Reads after quality control were mapped to the representative genes with 95% identities using SOAPaligner (http://soap.genomics.org.cn/), and gene abundance in each sample was evaluated.

Differences analysis in microbiota composition

The linear discriminant analysis (LDA) Effect Size (LEfSe) was used to support high-dimensional group comparisons to find biological relevant characteristics. First, the non-parametric factorial kruskal-wallis sum-rank test was used to detect features with significant differential abundance between groups, with biological consistency investigated among subgroups using the Wilcoxon rank-sum test. Finally, the above-obtained data were used for LDA model analysis to rank the relative abundance difference with respect to groups. The significance for each test was set to 0.05.

Analysis of microbiome functional composition

The Venn diagram can be used to count the number of common and unique functions in multiple groups of samples. The relationship diagram of Circos samples and function is a visual circle diagram describing the corresponding relationship between samples and function, which not only reflects the composition ratio of dominant function of each sample, but also reflects the distribution ratio of each dominant function among different samples. In MAP, MSAP, and SAP, Venn diagram and Circos diagram were respectively used to analyze the functional composition of microbiota and the relationship between samples and microbiota functional composition by using R language.

Species annotation of microbiome in the amino acid sequence of non-redundant (NR) proteins database

The NR gene set was compared with the NR database using DIAMOND (http://ab.inf.uni-tuebingen.de/software/diamond/) software to obtain through taxonomic information in the NR database. The species abundance was calculated and counted in various taxonomic level including the Domain, Kingdom, Phylum, Class, Order, Family, Genus and Species to build corresponding taxonomic level abundance of spectrum (abundance profile).

Functional annotation of microbiome in the clusters of orthologous groups of proteins (COG) database

BLASTP (http://blast.ncbi.nlm.nih.gov/Blast.cgi) (Version 2.2.28+) was employed for taxonomic annotations by aligning non-redundant gene catalogs against NCBI NR database with an e-value cutoff of 1e-5. Cluster of orthologous groups of proteins (COG) for the ORFs annotation was performed using BLASTP against eggNOG database (v4.5) with an e-value cutoff of 1e-5.

Functional annotation of microbiome in the kyoto encyclopedia of genes and genomes (KEGG) database

The KEGG pathway annotation was conducted using BLASTP search (http://blast.ncbi.nlm.nih.gov/Blast.cgi) (Version 2.2.28+) against the KEGG (http://www.genome.jp/keeg/) with an e-value cutoff of 1e-5.

Functional annotation of microbiome in the carbohydrate active enzymes (CAZy) database

According to the similarity of amino acid sequence, carbohydrate active enzyme from different species can be divided into carbohydrates glycoside hydrolase (GHs), glycosyl transferase (GTs), polysaccharide lyase (PLs), carbohydrate esterases (CEs), carbohydrate binding modules (CBMs), auxiliary activities (AAs) and other six major protein families. Carbohydrate-active enzymes annotation was conducted using hmmscan (http://hmmer.janelia.org/search/hmmscan) against CAZy database V5.0 (http://www.cazy.org/) with an e-value cutoff of 1e-5.

Functional annotation of microbiome in the Antibiotic Resistance Genes Database (ARDB)

The ARDB (http://ardb.cbcb.umd.edu/) database includes bacterial resistance genes from different environmental sources (such as the intestinal tract), and their resistance spectra, mechanism of action, ontology and other annotation information, providing research basis for the study of drug action. Functional annotation was conducted using BLASTP search (Version 2.2.28+) against ARDB database (http://ardb.cbcb.umd.edu/) with an e-value cutoff of 1e-5.

Functional annotation of microbiome in the comprehensive antibiotic resistance database (CARD)

CARD (http://arpcard. Mcmaster.ca) database contains a wide range of antibiotic resistance-related reference genes from a variety of organisms, genomes and plasmids, which can be used to guide the study of antibiotic resistance mechanisms in human and animal flora groups. Functional annotation was conducted using BLASTP search (Version 2.2.28+) against CARD database (http://ardb.cbcb.umd.edu/) with an e-value cutoff of 1e-5.

Functional annotation of microbiome in the virulence factor database (VFDB)

The VFDB (http://www.mgc.ac.cn/VFs/) is a comprehensive integrated network database for pathogen virulence factor information management. Functional annotation was conducted using BLASTP search (Version 2.2.28+) against VFDB database (http://www.mgc.ac.cn/VFs/) with an e-value cutoff of 1e-5.

Analysis of microbiotafunctional composition difference

Based on the functional composition abundance data, relevant analysis methods were used to detect the functional composition diversity of microbial communities. In this study, the significance test was used to screen different functional compositions of microbiota in MAP, MSAP, and SAP. Detailed screening process was as follows: 1) Wilcoxon rank-sum test was used to test the average rank of the two groups of samples and determine whether there were differences in the distribution of the two samples; 2) multiple inspection and correction method for P value (FDR) was applied; 3) double tail test was used to specify the type of confidence interval desired; 4) Welch T test was used to calculate the confidence interval (confidence: 0.95); 5) The screening criteria is $p<0.05$.

Results

Clinical characteristics of patients and healthy subjects

A total of 9 AP patients (3 MAP, 3 MSAP, and 3 SAP) and 3 HCR were enrolled in this study. The HCR group were all women and they were 42.0±14.2 years old with a BMI of 20.9±2.3. The clinical characteristics of AP groups were shown in Table 1. Age (p=0.473) and gender (p=0.99) were comparable between the AP groups and the HCR group. Among the AP patients statistically significant differences were observed in local complications, duration of organ failure, ICU admission, length of ICU stay, and length of hospital stay (Table 1). None of the AP patients died.

Differences analysis in microbiota composition

In MAP, the taxa of *Thermoprotei* and *Crenarchaeota* was significantly more enriched compared to HCR (supplementary Figure 1A). *Sulfolobus* was remarkably more abundant in MSAP compared to HCR (supplementary Figure 1B). In SAP, enrichment in the taxa of *Sulfolobales* was significantly observed compared to HCR (supplementary Figure 1C). *Methanobrevibacter_ruminantium* and *Methanosarcina_thermophila* were uniquely abundant in MSAP compared to MAP (supplementary Figure 1D). *Methanomicrobiales_archaeon_53_19* was remarkably abundant in SAP compared to MSAP (supplementary Figure 1E).

Analysis of microbiome functional composition

The Venn diagram showed that KEGG was the most enriched functional composition in MAP (supplementary Figure 2A). CAZy and VFDB were the most enriched functional compositions in MSAP (supplementary Figure 2B). From the Circos diagram, we found that macrolide was dominant functional composition of ARDB in MAP (supplementary Figure 3A); *Escherichia-coli* was the dominant microbiota specie of NR in MSAP (supplementary Figure 3B); In SAP, GT4 (glucosyltransferase) was a dominant functional composition of CAZy (supplementary Figure 3C).

Difference analysis of microbiotafunctional composition of NR

In the analysis of NR functional composition, there were 364, 181, and 133 significantly different microbiota species in MAP, MSAP, and SAP, respectively. *Streptococcus* and *Anaerostipes hadrus* was respectively the most significantly increased (p=0.01211) and decreased (p=0.0009861) microbiota species in MAP (supplementary Figure 4A). Unclassified *Bacteria* and *Anaerostipes hadrus* was respectively the most significantly increased (p=0.01912) and decreased (p=0.001623) microbiota species in MSAP (Figure 4B). In SAP, *Enterococcus* and *Blautia* was respectively the most significantly increased (p=0.03043) and decreased (p=0.001954) microbiota species (Figure 4C).

Difference analysis of microbiotafunctional composition of COG

In the analysis of COG functional composition, there were 0, 5, and 3 significantly different functional compositions in MAP, MSAP, and SAP, respectively. U (intracellular trafficking, secretion, and vesicular transport) and Z (cytoskeleton) was respectively the most significantly increased (p=0.002019) and

decreased (p=0.02135) COG functional composition in MSAP (Figure 1A). In SAP, C (energy production and conversion) and T (signal transduction mechanisms) was respectively the most significantly increased (p=0.03573) and decreased (p=0.01441) COG functional composition (Figure 1B).

Difference analysis of microbiotafunctional composition of KEGG

In the analysis of KEGG functional composition, there were 21, 37, and 27 significantly different functional compositions in MAP, MSAP, and SAP, respectively. Glutathione metabolism and Neomycin, kanamycin and gentamicin biosynthesis was respectively the most significantly increased (p=0.0005001) and decreased (p=0.004317) KEGG functional composition in MAP (Figure 2A). Lipopolysaccharide biosynthesis and starch and sucrose metabolism was respectively the most significantly increased (p=0.006658) and decreased (p=0.0007967) KEGG functional composition in MSAP (Figure 2B). In SAP, valine, leucine and isoleucine degradation and fatty acid metabolism was respectively the most significantly increased (p=0.00221) and decreased (p=0.0002432) KEGG functional composition (Figure 2C).

Difference analysis of microbiotafunctional composition of CAZy

In the analysis of CAZy functional composition, there were 15, 11, and 11 significantly different functional compositions in MAP, MSAP, and SAP, respectively. GT41 (glycosidyltransferase) and GH109 (glycoside hydrolase) was respectively the most significantly increased (p=0.01794) and decreased (p=0.003512) CAZy functional composition in MAP (Figure 3A). GH13_12 (glycoside hydrolase) and GH13_19 (glycoside hydrolase) was respectively the most significantly increased (p=0.04356) and decreased (p=0.01145) CAZy functional composition in MSAP (Figure 3B). In SAP, GH120 (glycoside hydrolase) was the most significantly decreased (p=0.003314) CAZy functional composition (Figure 3C).

Difference analysis of microbiotafunctional composition of ARDB

In the analysis of ARDB functional composition, there were 2, 22, and 2 significantly different functional compositions in MAP, MSAP, and SAP, respectively. Gentamicin was the most significantly increased (p=0.005638) ARDB functional composition in MAP (Figure 4A). Penicillin and bacitracin was respectively the most significantly increased (p=0.0006484) and decreased (p=0.02834) ARDB functional composition in MSAP (Figure 4B). In SAP, tetracycline was the most significantly decreased (p=0.009731) ARDB functional composition (Figure 4C).

Difference analysis of microbiotafunctional composition of CARD

In the analysis of CARD functional composition, there were 27, 48, and 25 significantly different functional compositions in MAP, MSAP, and SAP, respectively. ARO: 3003830 (aminocoumarin antibiotic) and ARO: 3003728 (glycopeptide antibiotics) was respectively the most significantly increased (p=0.007521) and decreased (p=0.002542) CARD functional composition in MAP (Figure 5A). ARO: 3003835 (fluoroquinolone antibiotics) was the most significantly decreased (p=0.005962) CARD

functional composition in MSAP (Figure 5B). In SAP, ARO: 3003770 (peptide antibiotics) was the most significantly increased (p=0.00179) CARD functional composition (Figure 5C).

Difference analysis of microbiotafunctional composition of VFDB

In the analysis of VFDB functional composition, there were 55, 107, and 55 significantly different functional compositions in MAP, MSAP, and SAP, respectively. FeoAB was the most significantly decreased (p=0.005331) VFDB functional composition in MAP (Figure 6A). Capsular polysaccharide and Two-component system was respectively the most significantly increased (p=0.0002623) and decreased (p=0.004764) VFDB functional composition in MSAP (Figure 6B). In SAP, alginate biosynthesis and Two-component system were respectively the most significantly increased (p=0.003317) and decreased (p=0.0008046) VFDB functional composition (Figure 6C).

Discussion

In this study, we performed the Shotgun metagenomic sequencing approach to a cohort of 12 individuals, including 9 AP patients (3 MAP, 3 MSAP, and 3 SAP) and 3 HCR. We found remarkably different outcomes (table 1) and significant dysbiosis of microbiome composition and function in the AP patients. Moreover, the composition and function of microbiota in SAP were different from MAP and MSAP, implying the association of the dysbiosis of microbial composition and function to AP severity.

Firstly, in differences analysis in microbiota composition, we found that *Thermoprotei* and *Crenarchaeota* were significantly enriched in MAP; and *Sulfolobus* was highly abundant in MSAP and SAP. We also found that *Methanobrevibacter_ruminantium* and *Methanosarcina_thermophila* were uniquely abundant in MSAP compared to MAP, and *Methanomicrobiales_archaeon_53_19* was highly abundant in SAP compared to MSAP. *Methanobrevibacter* is a major intestinal methanogenic archaeon [14]. Gaci N et al. reported that the mammalian gut is occupied by methanogenic archeaea such as *methanomicrobiales* [15]. The *methanomicrobiales* was also detected in fecal samples in foals [16]. This was the first time for microbiotas to be identified in AP patients. Further mechanism research is needed.

In the differential analysis of microbiota composition, we found that *Streptococcus* and *Anaerostipes hadrus* were respectively the most significantly increased and decreased microbiota species in MAP; *Anaerostipes hadrus* was the most significantly decreased microbiota species in MSAP. In addition, from the Circos diagram, we found that *Escherichia-coli* was the dominant microbiota specie in MSAP. *Streptococcus*, a type of Gram-positive bacteria, is a common pathogen in infected pancreatitis necrosis [17]. It has also been reported that *Streptococcus* is related to chronic alcoholic pancreatitis and pancreatic cancer [18]. *Anaerostipes hadrus* converts indigestible carbohydrates into fermentation products, including short-chain fatty acids (SCFAs, such as butyrate) [19]. Since SCFA is essential in maintaining gut barrier, host metabolism and immunity, the reduction of SCFAs-producing bacteria can be detrimental in patients with AP. It is not surprising that *Anaerostipes hadrus* is associated with the pathogenesis of chronic alcoholic pancreatitis [20]. *Escherichia-coli* is the predominant microbiotas in pancreatic cyst fluids and consists a common pathogen of infected pancreatic necrosis in non-mild AP

[21]. Our findings suggested that the alteration of microbiotas may play roles in the development of MAP and MSAP.

In SAP, we found that *Enterococcus* and *Blautia* were respectively the most significantly increased and decreased microbiota species. Previous studies have demonstrated that *Enterococcus* could adhere and invade the surface of host cells, cross host epithelial barriers, and get access to other organs and the systemic circulation, leading to sepsis and organ failure [7]. The relative abundance of *Enterococcus* (potential harmful pathogens) is related to infection and systemic inflammation in patients with AP [22]. The inoculation of *Il10-/-* mice with *Enterococcus* species causes characteristic chronic inflammatory diseases, supporting its pathogenic role [23]. It is also found that the population of intestinal *Enterococcus* is higher in the gut flora of SAP patients [24]. *Blautia* is the predominant taxa (beneficent microbiota) in the intestinal tract of the healthy population [25]. Significant reduction of *Blautia* levels in patients with SAP, as revealed in this study, promotes the overgrowth of intestinal bacteria, increases intestinal permeability, and ultimately results in higher concentrations of endotoxins and activation of inflammatory cascades [9] . These findings altogether indicated that the disbalance of *Enterococcus* and *Blautia* might play a key role in the inflammatory process of SAP.

Besides the dysbiosis of microbiome composition, we also found microbial dysfunction in AP patients. In differential analysis, we revealed that intracellular trafficking, secretion, and vesicular transport and cytoskeleton was the most significantly altered COG functional composition in MSAP. It is reported that disruption of polarized intracellular trafficking may leads to interstitial leakage of pancreatic enzymes and other macromolecules, and finally pancreatitis [26]. In the acinar cell, undefined intracellular trafficking defects and secretory blockade are believed to culminate in pathologic proenzyme activation during AP [27]. AP induced by supramaximal secretagogue stimulation is characterized by the early and rapid disruption of the apical actin cytoskeleton [28]. Our result is consistent with that of Jungermann J and Ueda T et al., and they found that the tubulin cytoskeleton was disrupted in an experimental model of AP [29, 30]. In SAP, we found that energy production and conversion was the most significantly increased COG functional composition. The gut microbiota plays a crucial role in energy metabolism to maintain the host homeostasis [31]. On account of acute systemic inflammatory response syndrome, AP (especially SAP) always triggers a hypercatabolic state, resulting in increased energy requirements [32]. Our result further suggested the important roles of intracellular trafficking, secretion, cytoskeleton, and energy metabolism in the process of MSAP and SAP.

In differential analysis, we found that glutathione metabolism was the most significantly increased KEGG functional composition in MAP. Glutathione system assists certain pathogens' survival in inflammatory tissues [33]. Previous studies showed that changes in glutathione metabolism occurred at the early stage of acute pancreatitis [34]. In addition, we found that lipopolysaccharide biosynthesis and starch and sucrose metabolism was the most significantly increased and decreased KEGG functional composition in MSAP. Lipopolysaccharide damages the intestinal barrier, which in turn increases mucosal permeability and promotes bacterial translocation [35]. Lipopolysaccharide also induces early damage and remarkable inflammation in the pancreas [36]. Raetz CR and Exley AR et al. detected the existence of

lipopolysaccharides in the plasma of patients with SAP at an early stage of the disease [37, 38]. In healthy individuals, the starch that entered the large bowel is metabolized by various saccharolytic bacteria (inhabiting that region of the intestine), which in turn promote the production of SCFA [39]. In patients with SAP, we found that valine, leucine, and isoleucine degradation and fatty acid metabolism was the most significantly increased and decreased KEGG functional composition. Valine can be used to accurately discriminate hyperlipidemic AP from healthy controls [40]. The level of valine is significantly decreased in the serum of chronic pancreatitis patients [41]. Some authors believed that valine could be a potential biomarker for early-stage AP [42]. Leucine and isoleucine has been found in the serum of patients with chronic pancreatitis [41]. In pancreatitis, excess free fatty acids cause oxidative stress, free radical accumulation, and acinar necrosis [43]. Saharia P and Halangk W et al. reported that perfusion of mice pancreas with fatty acid induced pancreatic edema could activate trypsinogen, which ultimately initiate AP [44, 45]. Of note is that high amounts of unsaturated fatty acids have been detected in the serum of SAP patients [46]. Our study indicated that the above microbiota functional compositions of KEGG might be involved in the pathogenesis and progression of AP.

Furthermore, we found that GT41 (glycosidyltransferase) was the most significantly increased CAZy functional composition in MAP. In addition, from the analysis of microbiome functional composition (Circos diagram), we found that GT4 (glucosyltransferase) was a dominant functional composition of CAZy in SAP. It is reported that the glucosyltransferase activity of the toxin impacts secretion of inflammatory mediators [47]. This suggested that glycosidyltransferase may play a key role in the inflammatory response of MAP and SAP. We also showed that gentamicin was the most significantly increased ARDB functional composition in MAP. From the analysis of microbiome functional composition (Circos diagram), we found that macrolide was a dominant functional composition of ARDB in MAP. Gentamicin is a macrolide prescribed for infected necrosis in AP patients [48]. Macrolides have a number of biological effects potentially beneficial for AP, including antibacterial and anti-inflammatory activity [49, 50]. In MSAP, we found that penicillin was the most significantly increased ARDB functional composition. Penicillin is considered a Class IV drug that could induce AP [51]. It has been demonstrated that penicillin is ineffective in treating patients with AP [52]. In addition, we found that tetracycline was the most significantly decreased ARDB functional composition in SAP. In fact, tetracycline has been claimed to increase the risk of AP and is ineffective in treating AP [52, 53]. In this study, we found the microbial resistance in MAP, MSAP, and SAP, which suggested that gentamicin, macrolide and tetracycline would not be considered as optimal therapeutic drugs for infectious complications of AP.

In the differential analysis of microbiota functional composition of CARD, we found that aminocoumarin antibiotic and glycopeptide antibiotic was the most significantly increased and decreased CARD functional composition in MAP. 3-Aminocoumarin derivatives possess a number of biological activities, such as antibacterial. The N-glycopeptides is identified in the pancreas tissue [54]. Some N-glycopeptides are elevated in chronic pancreatitis [55]. In MSAP, we found that fluoroquinolone antibiotic was the most significantly decreased CARD functional composition. Fluoroquinolone has adequate tissue penetration and bactericidal properties in infected pancreatic necrosis [56]. Clinically, fluoroquinolone has been recommended for antimicrobial therapy in AP [57]. Our findings indicated that microbial resistance to

aminocoumarin, glycopeptides and fluoroquinolone antibiotics in MAP and MSAP may provide the research basis for the study of drug action in AP.

In the differential analysis of microbiota functional composition of VFDB, we found that FeoAB was the most significantly decreased VFDB functional composition in MAP. The *feoAB* operon of *Escherichia coli* is the most-characterized ferrous iron transport system, which promotes intracellular infection [58]. In MSAP, we found that capsular polysaccharide was the most significantly increased VFDB functional composition. Several pathogenic bacteria, such as *Escherichia-coli* could produce capsular polysaccharide known as glycosaminoglycans for molecular camouflage [59]. Maekawa T et al. found that patients with chronic pancreatitis were characterized by increased serum level of antibody against the capsular polysaccharide of *Enterococcus faecalis* [60]. In addition, we found that two-component system was the most significantly decreased VFDB functional composition in both MSAP and SAP. It is reported that peptidoglycan recognition proteins bind to the outer membrane of *Escherichia coli* and activates functionally homologous CpxA-CpxR two-component system, which modulates microbiome and inflammation [61]. Our study suggested that above virulent factors, including FeoAB, capsular polysaccharide, and the two-component system, may promote microbial infection and cause AP.

Conclusions

We conducted a shotgun metagenomics survey on the gut microbiome of AP patients with three different severity grades for the first time. We identified several new AP-related bacteria and functional gene pathways, which extend the current knowledge about the role of gut microbiota in AP. Our findings may be useful for future studies investigating the worsening mechanism of AP and developing strategies for the prevention, diagnosis, and treatment of AP. Needless to say that there are certain limitations in our study. Firstly, the sample size is small, and further longitudinal studies with a larger number of subjects are needed. Secondly, causal links between these microbiota and functional pathways and AP susceptibility need a deeper investigation.

Abbreviations

AP: acute pancreatitis; ARDB: antibiotic resistance genes database; AAs: auxiliary activities; CAZy: carbohydrate active enzymes; CBMs: carbohydrate binding modules; CEs: carbohydrate esterases; CARD: comprehensive antibiotic resistance database; GHs: glycoside hydrolase; GTs: glycosyl transferase; KEGG: kyoto encyclopedia of genes and genomes; LDA: linear discriminant analysis; LEfSe: linear discriminant analysis effect size; MAP: mild acute pancreatitis; MSAP: moderately severe acute pancreatitis; NR: non-redundant; HCR: healthy control population; ORFs: open reading frames; COG: orthologous groups of proteins; PLs: polysaccharide lyase; SAP: severe acute pancreatitis; VFDB: virulence factor database

Declarations

All the authors declared no conflict of interest.

Ethics approval and consent to participate

Written informed consent was obtained from each participant. The institutional review boards of Peking Union Medical College Hospital approved this study (No. JS 1826).

Consent for publication

All the authors have consented for publication of this paper in the current form.

Availability of data and material

All data generated or analyzed during this study are included in this published article.

Competing interests

The authors declare that they have no competing interests.

Funding

This work was supported by the Beijing Natural Science Foundation (No. 7192162) and Chinese Academy of Medical Sciences（Beijing） (2019XK320036).

Authors' contributions

YSS, XYY and FYY contributed to collection of clinical data and fecal samples, and interpretation of data, and drafting of the article. WD, MX, and XJ contributed to the concept and design of the study, interpretation of data, and the critical revision of the study methods. CGR contributed to the critical revision of the article for relevant intellectual content. ZHD made critical review of the article for valuable intellectual content. WD and XJcontributed to the drafting of the article, and critical revision of the article. All authors approved the final version of the article, including the authorship list.

Acknowledgements

The authors want to thank Dr. Zhang Yan for the editing of this paper.

References

1. Pendharkar SA, Salt K, Plank LD, Windsor JA, Petrov MS: **Quality of life after acute pancreatitis: a systematic review and meta-analysis.***Pancreas* 2014, **43:**1194-1200.
2. Garg SK, Sarvepalli S, Campbell JP, Obaitan I, Singh D, Bazerbachi F, Singh R, Sanaka MR: **Incidence, Admission Rates, and Predictors, and Economic Burden of Adult Emergency Visits for Acute Pancreatitis: Data From the National Emergency Department Sample, 2006 to 2012.***J Clin Gastroenterol* 2019, **53:**220-225.

3. Banks PA, Bollen TL, Dervenis C, Gooszen HG, Johnson CD, Sarr MG, Tsiotos GG, Vege SS: **Classification of acute pancreatitis–2012: revision of the Atlanta classification and definitions by international consensus.** *Gut* 2013, **62:**102-111.
4. Wu D, Lu B, Xue HD, Yang H, Qian JM, Lee P, Windsor JA: **Validation of Modified Determinant-Based Classification of severity for acute pancreatitis in a tertiary teaching hospital.** *Pancreatology* 2019, **19:**217-223.
5. Jin M, Bai X, Chen X, Zhang H, Lu B, Li Y, Lai Y, Qian J, Yang H: **A 16-year trend of etiology in acute pancreatitis: The increasing proportion of hypertriglyceridemia-associated acute pancreatitis and its adverse effect on prognosis.** *J Clin Lipidol* 2019, **13:**947-953.e941.
6. Desai MS, Seekatz AM, Koropatkin NM, Kamada N, Hickey CA, Wolter M, Pudlo NA, Kitamoto S, Terrapon N, Muller A, et al: **A Dietary Fiber-Deprived Gut Microbiota Degrades the Colonic Mucus Barrier and Enhances Pathogen Susceptibility.** *Cell* 2016, **167:**1339-1353.e1321.
7. Zhu Y, He C, Li X, Cai Y, Hu J, Liao Y, Zhao J, Xia L, He W, Liu L, et al: **Gut microbiota dysbiosis worsens the severity of acute pancreatitis in patients and mice.** *J Gastroenterol* 2019, **54:**347-358.
8. Li Q, Wang C, Tang C, He Q, Li N, Li J: **Bacteremia in patients with acute pancreatitis as revealed by 16S ribosomal RNA gene-based techniques*.** *Crit Care Med* 2013, **41:**1938-1950.
9. Yu S, Xiong Y, Xu J, Liang X, Fu Y, Liu D, Yu X, Wu D: **Identification of Dysfunctional Gut Microbiota Through Rectal Swab in Patients with Different Severity of Acute Pancreatitis.** 2020.
10. Abubucker S, Segata N, Goll J, Schubert AM, Izard J, Cantarel BL, Rodriguez-Mueller B, Zucker J, Thiagarajan M, Henrissat B, et al: **Metabolic reconstruction for metagenomic data and its application to the human microbiome.** *PLoS Comput Biol* 2012, **8:**e1002358.
11. Wang WL, Xu SY, Ren ZG, Tao L, Jiang JW, Zheng SS: **Application of metagenomics in the human gut microbiome.** *World J Gastroenterol* 2015, **21:**803-814.
12. Singer M, Deutschman CS, Seymour CW, Shankar-Hari M, Annane D, Bauer M, Bellomo R, Bernard GR, Chiche JD, Coopersmith CM, et al: **The Third International Consensus Definitions for Sepsis and Septic Shock (Sepsis-3).** *Jama* 2016, **315:**801-810.
13. Bassis CM, Moore NM, Lolans K, Seekatz AM, Weinstein RA, Young VB, Hayden MK: **Comparison of stool versus rectal swab samples and storage conditions on bacterial community profiles.** *BMC Microbiol* 2017, **17:**78.
14. Eckburg PB, Bik EM, Bernstein CN, Purdom E, Dethlefsen L, Sargent M, Gill SR, Nelson KE, Relman DA: **Diversity of the human intestinal microbial flora.** *Science* 2005, **308:**1635-1638.
15. **Archaea and the human gut:New beginning of an old story.** *World Journal of Gastroenterology***:**137-153.
16. Bordin AI, Suchodolski JS, Markel ME, Weaver KB, Steiner JM, Dowd SE, Pillai S, Cohen ND: **Effects of Administration of Live or Inactivated Virulent Rhodococccus equi and Age on the Fecal Microbiome of Neonatal Foals.** *Plos One* 2013, **8**.
17. **Focused open necrosectomy in necrotizing pancreatitis.** *HPB* 2013, **15**.

18. Farrell JJ, Zhang L, Zhou H, Chia D, Elashoff D, Akin D, Paster BJ, Joshipura K, Wong DT: **Variations of oral microbiota are associated with pancreatic diseases including pancreatic cancer.***Gut* 2012, **61:**582-588.
19. Eeckhaut V, Van Immerseel F, Pasmans F, De Brandt E, Haesebrouck F, Ducatelle R, Vandamme P: **Anaerostipes butyraticus sp. nov., an anaerobic, butyrate-producing bacterium from Clostridium cluster XIVa isolated from broiler chicken caecal content, and emended description of the genus Anaerostipes.***Int J Syst Evol Microbiol* 2010, **60:**1108-1112.
20. Ciocan D, Rebours V, Voican CS, Wrzosek L, Perlemuter G: **Characterization of intestinal microbiota in alcoholic patients with and without alcoholic hepatitis or chronic alcoholic pancreatitis.***Scientific Reports* 2018, **8**.
21. Li S, Fuhler GM, BN N, Jose T, Bruno MJ, Peppelenbosch MP, Konstantinov SR: **Pancreatic cyst fluid harbors a unique microbiome.***Microbiome*, **5:**147.
22. Marshall JC, Christou NV, Horn R, Meakins JL: **The Microbiology of Multiple Organ Failure: The Proximal Gastrointestinal Tract as an Occult Reservoir of Pathogens.** 1988, **123:**309-315.
23. Bianca K, Marcus D, Zhu S, Cookson AL, Mcnabb WC, Barnett Matthew PG, Katia N, Hodgkinson AJ, Roy NC: **Changes in colon gene expression associated with increased colon inflammation in interleukin-10 gene-deficient mice inoculated with Enterococcus species.***Bmc Immunology* 2010, **11:**1-21.
24. Tan C, Ling Z, Huang Y, Cao Y, Keqian XU: **Dysbiosis of Intestinal Microbiota Associated With Inflammation Involved in the Progression of Acute Pancreatitis.***Pancreas* 2014.
25. Falony G, Joossens M, Vieira-Silva S, Wang J, Darzi Y, Faust K, Kurilshikov A, Bonder MJ, Valles-Colomer M, Vandeputte D: **Population-level analysis of gut microbiome variation.***Science*, **352:**560-564.
26. Gaisano HY, Lutz MP, Leser J, Sheu L, Lynch G, Tang L, Tamori Y, Trimble WS, Salapatek AM: **Supramaximal cholecystokinin displaces Munc18c from the pancreatic acinar basal surface, redirecting apical exocytosis to the basal membrane.***J Clin Invest* 2001, **108:**1597-1611.
27. Waldron RT, Su H-Y, Piplani H, Capri J, Cohn W, Whitelegge JP, Faull KF, Sakkiah S, Abrol R, Yang W: **Ethanol Induced Disordering of Pancreatic Acinar Cell Endoplasmic Reticulum: An ER Stress/Defective Unfolded Protein Response Model.***Cellular & Molecular Gastroenterology & Hepatology*, **5:**479-497.
28. Weber H, Hühns S, Lüthen F, Jonas L: **Calpain-mediated breakdown of cytoskeletal proteins contributes to cholecystokinin-induced damage of rat pancreatic acini.***International Journal of Experimental Pathology* 2009, **90:**387-399.
29. Jungermann J, Lerch MM, Weidenbach H, Lutz MP, Krüger B, Adler G: **Disassembly of rat pancreatic acinar cell cytoskeleton during supramaximal secretagogue stimulation.** 1995, **268:**328-338.
30. Ueda T, Takeyama Y, Kaneda K, Adachi M, Saitoh Y: **Protective effect of a microtubule stabilizer Taxol on cerulein-induced acute pancreatitis in rat.***Journal of Clinical Investigation* 1992, **89:**234-243.

31. Tremaroli V, Backhed F: **Functional interactions between the gut microbiota and host metabolism.***Nature* 2012, **489:**242-249.
32. **UK guidelines for the management of acute pancreatitis.***Gut* 2005, **54 Suppl 3:**iii1-9.
33. Brenot A, King KY, Janowiak B, Griffith O, Caparon MG: **Contribution of Glutathione Peroxidase to the Virulence of Streptococcus pyogenes.***Infection & Immunity* 2004, **72:**408-413.
34. Schoenberg MH, Buchler M, Younes M, Kirchmayr R, Bruckner UB, Beger HG: **Effect of antioxidant treatment in rats with acute hemorrhagic pancreatitis.***Dig Dis Sci* 1994, **39:**1034-1040.
35. Berg RD: **Bacterial Translocation from the Gastrointestinal Tract.**
36. Leal AS, Sporn MB, Pioli PA, Liby KT: **The triterpenoid CDDO-imidazolide reduces immune cell infiltration and cytokine secretion in the KrasG12D;Pdx1-Cre (KC) mouse model of pancreatic cancer.***Carcinogenesis* 2016, **37:**1170-1179.
37. Raetz CR: **Bacterial endotoxins: extraordinary lipids that activate eucaryotic signal transduction.***J Bacteriol* 1993, **175:**5745-5753.
38. Exley AR, Leese T, Holliday MP, Swann RA, Cohen J: **Endotoxaemia and serum tumour necrosis factor as prognostic markers in severe acute pancreatitis.***Gut* 1992, **33:**1126-1128.
39. Topping DL, Clifton PM: **Short-chain fatty acids and human colonic function: roles of resistant starch and nonstarch polysaccharides.***Physiol Rev* 2001, **81:**1031-1064.
40. Tang M, Hu G, Zhao Y, Su M, Wang Y, Jia W, Qiu Y, Liu G, Wang X: **A serum metabolomic investigation on lipoprotein lipase-deficient mice with hyperlipidemic pancreatitis using gas chromatography/mass spectrometry.***Biomed Rep* 2013, **1:**469-473.
41. Adrych K, Smoczynski M, Stojek M, Sledzinski T, Swierczynski J: **Decreased serum essential and aromatic amino acids in patients with chronic pancreatitis.***World Journal of Gastroenterology* 2010, **16:**4422-4427.
42. Li J, Zhao XL, Liu YX, Peng XH, Zhu… SF: **1HNMR-based metabolomic profile of rats with experimental acute pancreatitis.***Bmc Gastroenterology*, **14**.
43. Ditzel J, Thaysen EH: **Increased hemoglobin-oxygen affinity in patients with pancreatitis associated with type I and V hyperlipoproteinemia.***Adv Exp Med Biol* 1977, **94:**423-428.
44. Saharia P, Margolis S, Zuidema GD, Cameron JL: **Acute pancreatitis with hyperlipemia: Studies with an isolated perfused canine pancreas.***Surgery* 1977, **82:**60-67.
45. Halangk W, Lerch MM, Brandt-Nedelev B, Roth W, Ruthenbuerger M, Reinheckel T, Domschke W, Lippert H, Peters C, Deussing J: **Role of cathepsin B in intracellular trypsinogen activation and the onset of acute pancreatitis.***Journal of Clinical Investigation*, **106:**773-781.
46. Domschke S, Malfertheiner P, Uhl W, Buchler M, Domschke W: **Free fatty acids in serum of patients with acute necrotizing or edematous pancreatitis.***Int J Pancreatol* 1993, **13:**105-110.
47. Cowardin CA, Jackman BM, Noor Z, Burgess SL, Feig AL: **Glucosylation Drives the Innate Inflammatory Response to Clostridium difficile Toxin A.** 2016, **84:**2317-2323.

48. Bassi C, Pederzoli P, Vesentini S, Falconi M, Bonora A, Abbas H, Benini A, Bertazzoni EM: **Behavior of antibiotics during human necrotizing pancreatitis.***Antimicrobial Agents & Chemotherapy*, **38:**830-836.
49. Schultz MJ: **Macrolide activities beyond their antimicrobial effects: macrolides in diffuse panbronchiolitis and cystic fibrosis.***J Antimicrob Chemother* 2004, **54:**21-28.
50. Kaurich T: **Drug-Induced Acute Pancreatitis.**
51. Badalov N, Baradarian R, Iswara K, Li J, Steinberg W, Tenner S: **Drug-Induced Acute Pancreatitis: An Evidence-Based Review.***Clinical Gastroenterology & Hepatology the Official Clinical Practice Journal of the American Gastroenterological Association*, **5:**648-661.e643.
52. Adarsh S, Moustafa M, Simon B: **Acute pancreatitis: current perspectives on diagnosis and management.***Journal of Inflammation Research*, **Volume 11:**77-85.
53. Nicolau DP, Mengedoht DE, Kline JJ: **Tetracycline-induced pancreatitis.***Am J Gastroenterol* 1991, **86:**1669-1671.
54. Pan S, Chen R, Tamura Y, Crispin DA, Lai LA, May DH, McIntosh MW, Goodlett DR, Brentnall TA: **Quantitative Glycoproteomics Analysis Reveals Changes in N-Glycosylation Level Associated with Pancreatic Ductal Adenocarcinoma.***Journal of Proteome Research*, **13:**1293-1306.
55. Pan S, Chen R, Stevens T, Bronner MP, May D, Tamura Y, McIntosh MW, Brentnall TA: **Proteomics portrait of archival lesions of chronic pancreatitis.***PLoS One* 2011, **6:**e27574.
56. Demetri GD, von Mehren M, Antonescu CR, DeMatteo RP, Ganjoo KN, Maki RG, Pisters PW, Raut CP, Riedel RF, Schuetze S, et al: **NCCN Task Force report: update on the management of patients with gastrointestinal stromal tumors.***J Natl Compr Canc Netw* 2010, **8 Suppl 2:**S1-41; quiz S42-44.
57. Haddad N, Kanj SS, Awad LS, Abdallah DI, Moghnieh RA: **The 2018 Lebanese Society of Infectious Diseases and Clinical Microbiology Guidelines for the use of antimicrobial therapy in complicated intra-abdominal infections in the era of antimicrobial resistance.***BMC Infectious Diseases* 2019.
58. Kammler M, Schon C, Hantke K: **Characterization of the ferrous iron uptake system of Escherichia coli.***J Bacteriol* 1993, **175:**6212-6219.
59. Ewald DR, Sumner SCJ: **Human microbiota, blood group antigens, and disease.***Wiley Interdisciplinary Reviews Systems Biology & Medicine***:**e1413.
60. Maekawa T, Fukaya R, Takamatsu S, Itoyama S, Fukuoka T, Yamada M, Hata T, Nagaoka S, Kawamoto K, Eguchi H, et al: **Possible involvement of Enterococcus infection in the pathogenesis of chronic pancreatitis and cancer.***Biochem Biophys Res Commun* 2018, **506:**962-969.
61. Dziarski R, Kashyap DR, Gupta D: **Mammalian peptidoglycan recognition proteins kill bacteria by activating two-component systems and modulate microbiome and inflammation.***Microb Drug Resist* 2012, **18:**280-285.

Tables

Table 1 The clinical characteristics of patients with acute pancreatitis

APFC: acute peripancreatic fluid collection; PPC: pancreatic pseudocyst; ARDS: acute

	MAP (n=3)	MSAP (n=3)	SAP (n=3)	F	P
Age (years)	67.3 ± 8.9	50.0 ± 25.2	57.0 ± 24.2	0.921	0.473
Male, n (%)	1 (33.3)	0 (0)	1 (33.3)	--	1.0
BMI	25.7 ± 2.2	26.3 ± 3.9[a]	24.6 ± 1.6		0.209
Smoking, n (%)	0 (0)	0 (0)	0 (0)	--	--
Etiology, n (%)				--	0.248
Biliary	0 (0)	1 (33.3)	1 (33.3)	--	--
Hyperlipidemia	3 (100)	1 (33.3)	2 (66.7)	--	--
Alcohol	0 (0)	1 (33.3)	0 (0)	--	--
APACHE II score	4.2 ± 1.2	4.7 ± 3.8	9.3 ± 4.2	2.13	0.234
Balthazar CT score ≧D n (%)	0 (0)	1 (33.3)	3 (100)	--	0.161
CRP (mg/L)	99.6 ± 26	123.7 ± 41.9	150.7 ± 16.2	2.188	0.193
Local complications, n (%)	0 (0)	3 (100)	3 (100)	--	0.035
APFC	0 (0)	3 (100)	3 (100)	--	0.036
PPC	0 (0)	0 (0)	2 (66.7)	--	0.251
Organ failure, n (%)	0 (0)	2 (66.7)	3 (100)	--	0.144
Duration of organ failure, hours	0	14.7 ± 15	116 ± 59.8[bc]		0.014
Systematic complications, n (%)	0 (0)	1 (33.3)	3 (100)	--	0.143
Shock	0 (0)	0 (0)	1 (33.3)	--	1.0
ARDS	0 (0)	2 (66.7)	1 (33.3)	--	0.68
AKI	0 (0)	1 (33.3)	1 (33.3)	--	1.0
AMS	0 (0)	0 (0)	1 (33.3)	--	1.0
ICU admission, n (%)	0 (0)	0 (0)	3 (100)	--	0.035
Length of ICU stay, days	0 (0)	0 (0)	9 (6)[bc]		0.017
Length of hospital stay, days	5 ± 2.5	10.7 ± 4.7	24 ± 5.2[bc]		0.001

respiratory distress syndrome; AMS: altered mental status; AKI: acute kidney injury; BMI: body mass index. a represents *P*<0.05 vs NOR; b represents *P*<0.05 vs MAP; c represents P<0.05 vs MSAP; –represents fisher test.

Figures

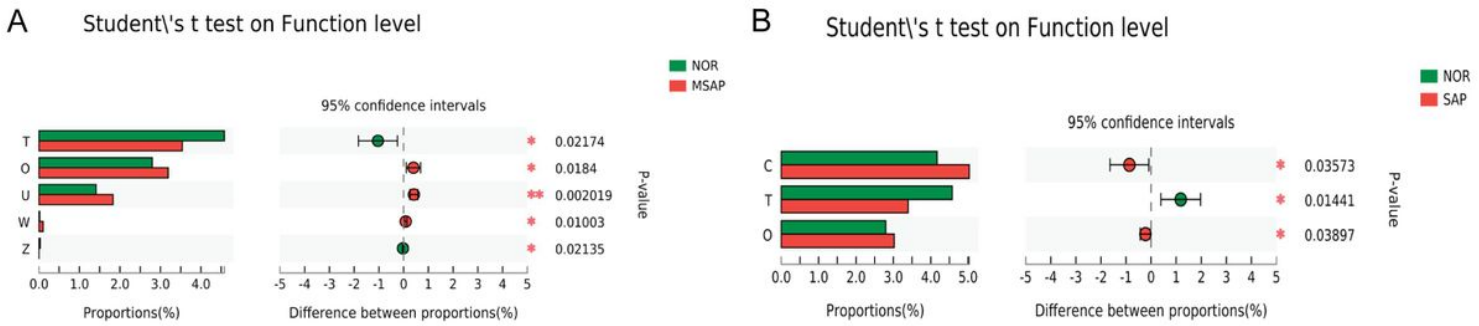

Figure 1

Difference analysis of COG functional composition in MSAP (A) and SAP (B) group. On the left, X and Y-axis represents the average relative abundance of the COG functional composition in various groups and the COG functional composition names at a certain classification level, respectively. On the right, X and Y axis represents different COG functional compositions between various groups and p-value of significance. *0.01<p<0.05, **0.01<p<0.001. U: intracellular trafficking, secretion, and vesicular transport; Z: cytoskeleton; C: energy production and conversion; T: signal transduction mechanisms; O: posttranslational modification, protein turnover, chaperones; W: extracellular structures.

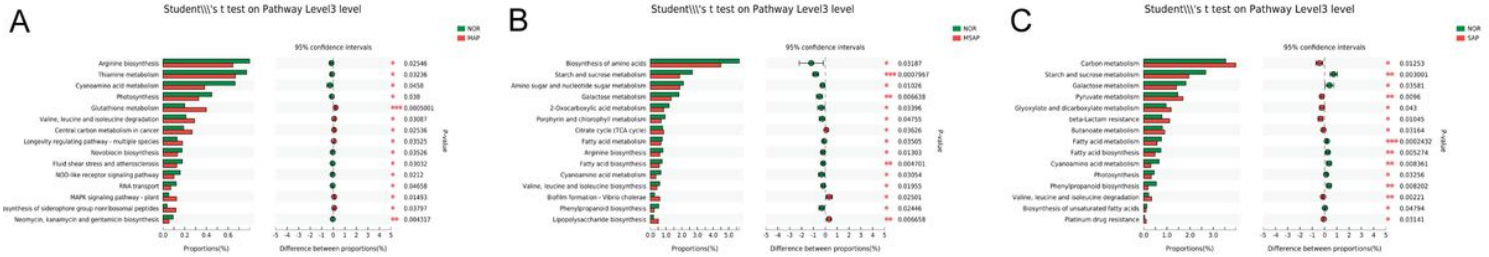

Figure 2

Difference analysis of KEGG functional composition in MAP (A), MSAP (B) and SAP (C) group. On the left, X and Y-axis represents the average relative abundance of the KEGG functional composition in various groups and KEGG functional composition names at a certain classification level, respectively. On the right, X and Y axis represents different KEGG functional compositions between various groups and p-value of significance. *0.01<p<0.05, **0.01<p<0.001, ***p<0.001.

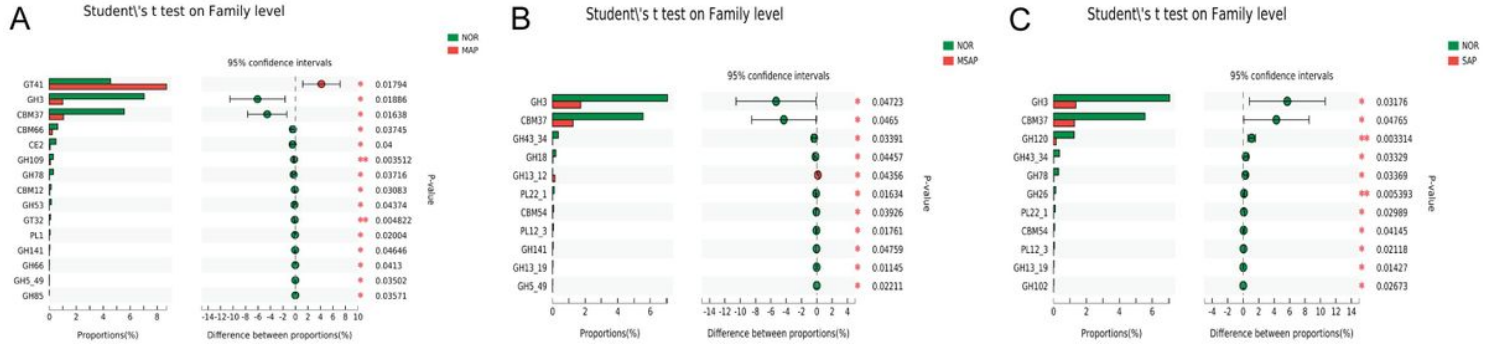

Figure 3

Difference analysis of CAZy functional composition in MAP (A), MSAP (B) and SAP (C) group. On the left, X and Y-axis represents the average relative abundance of the CAZy functional composition in various groups and the CAZy functional composition names at a certain classification level, respectively. On the right, X and Y axis represents different CAZy functional compositions between various groups and p-value of significance. *0.01<p<0.05, **0.01<p<0.001. GHs: glycoside hydrolases; GTs: glycosidyltransferases; PLs: polysaccharide lyases; CEs: carbohydrate lipases; CBMs: carbohydrate binding module.

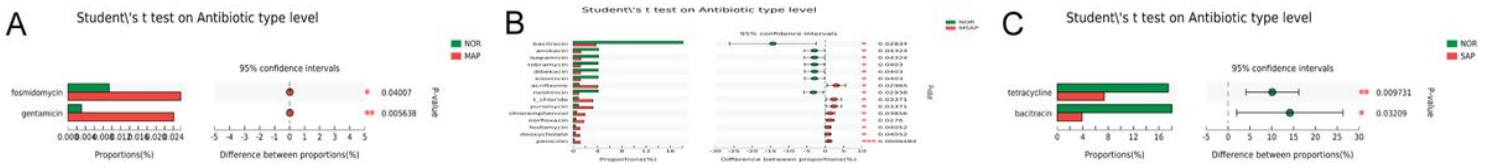

Figure 4

Difference analysis of ARDB functional composition in MAP (A), MSAP (B) and SAP (C) group. On the left, X and Y-axis represents the average relative abundance of the ARDB functional composition in various groups and the ARDB functional composition names at a certain classification level, respectively. On the right, X and Y axis represents different ARDB functional compositions between various groups and p-value of significance. *0.01<p<0.05, **0.01<p<0.001, ***p<0.001.

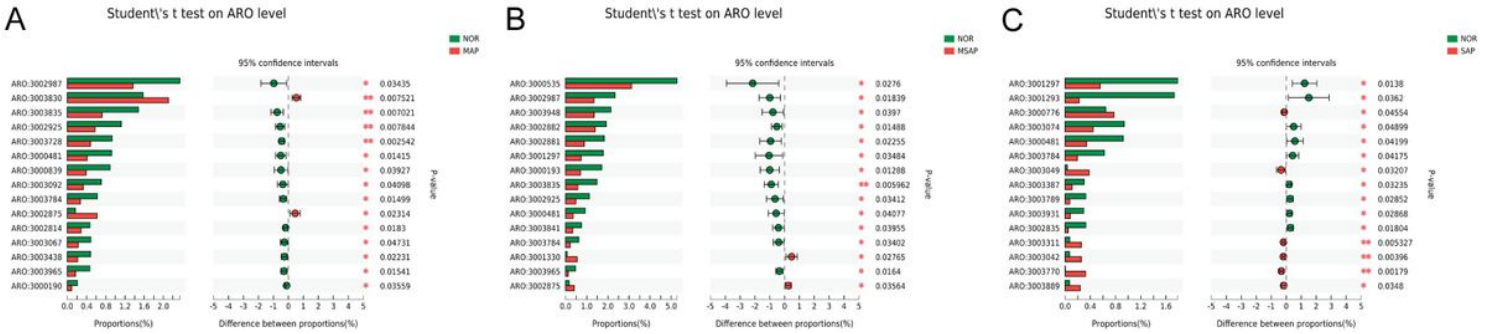

Figure 5

Difference analysis of CARD functional composition in MAP (A), MSAP (B) and SAP (C) group. On the left, X and Y-axis represents the average relative abundance of the CARD functional composition in various groups and the CARD functional composition names at a certain classification level, respectively. On the right, X and Y axis represents different CARD functional compositions between various groups and p-value of significance. *0.01<p<0.05, **0.01<p<0.001. Detailed annotation of each CARD functional composition name is available in the website of https://card.mcmaster.ca/ontology/39421.

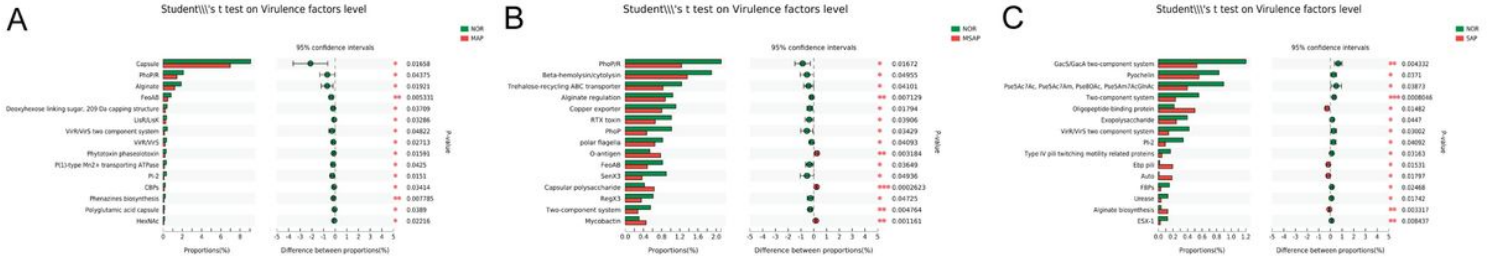

Figure 6

Difference analysis of VFDB functional composition in MAP (A), MSAP (B) and SAP (C) group. On the left, X and Y-axis represents the average relative abundance of the VFDB functional composition in various groups and the VFDB functional composition names at a certain classification level, respectively. On the right, X and Y axis represents different VFDB functional compositions between various groups and p-value of significance. *0.01<p<0.05, **0.01<p<0.001, ***p<0.001.

Supplementary Files

This is a list of supplementary files associated with this preprint. Click to download.

- SupplementaryFigure2A.png
- SupplementaryFigure2B.tif
- SupplementaryFigure1A.tif
- SupplementaryFigure2C.tif
- SupplementaryFigure1B.tif
- SupplementaryFigure1D.tif
- SupplementaryFigure4.tif
- SupplementaryFigure1E.tif
- SupplementaryFigure1C.tif
- SupplementaryFigure3A.tif
- SupplementaryFigure3C.tif
- SupplementaryFigure3B.tif